

Functional imaging to monitor vascular and metabolic response in canine head and neck tumors during fractionated radiotherapy

Jan Rødal, Espen Rusten, Åste Søvik, Hege Kippenes Skogmo & Eirik Malinen

To cite this article: Jan Rødal, Espen Rusten, Åste Søvik, Hege Kippenes Skogmo & Eirik Malinen (2013) Functional imaging to monitor vascular and metabolic response in canine head and neck tumors during fractionated radiotherapy, Acta Oncologica, 52:7, 1293-1299, DOI: [10.3109/0284186X.2013.812800](https://doi.org/10.3109/0284186X.2013.812800)

To link to this article: <https://doi.org/10.3109/0284186X.2013.812800>

 View supplementary material [↗](#)

 Published online: 23 Jul 2013.

 Submit your article to this journal [↗](#)

 Article views: 870

 View related articles [↗](#)

 Citing articles: 1 View citing articles [↗](#)

ORIGINAL ARTICLE

Functional imaging to monitor vascular and metabolic response in canine head and neck tumors during fractionated radiotherapy

JAN RØDAL¹, ESPEN RUSTEN^{1,2}, ÅSTE SØVIK³, HEGE KIPPENES SKOGMO³
& EIRIK MALINEN^{1,2}

¹Department of Medical Physics, Oslo University Hospital, Oslo, Norway, ²Department of Physics, University of Oslo, Norway and ³Department of Companion Animal Clinical Sciences, Norwegian School of Veterinary Science, Oslo, Norway

Abstract

Radiotherapy causes alterations in tumor biology, and non-invasive early assessment of such alterations may become useful for identifying treatment resistant disease. The purpose of the current work is to assess changes in vascular and metabolic features derived from functional imaging of canine head and neck tumors during fractionated radiotherapy. *Material and methods.* Three dogs with spontaneous head and neck tumors received intensity-modulated radiotherapy (IMRT). Contrast-enhanced cone beam computed tomography (CE-CBCT) at the treatment unit was performed at five treatment fractions. Dynamic ¹⁸F-FDG-PET (D-PET) was performed prior to the start of radiotherapy, at mid-treatment and at 3–12 weeks after the completion of treatment. Tumor contrast enhancement in the CE-CBCT images was used as a surrogate for tumor vasculature. Vascular and metabolic tumor parameters were further obtained from the D-PET images. Changes in these tumor parameters were assessed, with emphasis on intra-tumoral distributions. *Results.* For all three patients, metabolic imaging parameters obtained from D-PET decreased from the pre- to the inter-therapy session. Correspondingly, for two of three patients, vascular imaging parameters obtained from both CE-CBCT and D-PET increased. Only one of the tumors showed a clear metabolic response after therapy. No systematic changes in the intra-tumor heterogeneity in the imaging parameters were found. *Conclusion.* Changes in vascular and metabolic parameters could be detected by the current functional imaging methods. Vascular tumor features from CE-CBCT and D-PET corresponded well. CE-CBCT is a potential method for easy response assessment when the patient is at the treatment unit.

Assessment of tumor response is important with respect to evaluating the efficacy of a given treatment, in particular when introducing novel therapy regimens. Longitudinal tumor volume measurement is the conventional method for such assessments [1]. However, although the treatment may be effective, there are many tumor types where the volume changes slowly [2], making short-term response evaluation difficult. Thus, there is a need for methods that look for biological rather than anatomical features, as biological alterations precede tumor shrinkage.

Functional medical imaging comprises non-invasive methods for measuring and depicting biological processes in the living body. Contrast-enhanced computed tomography (CT) and magnetic resonance imaging (MRI), either in static or dynamic mode, provides images largely reflecting vascular

status [3,4]. Positron emission tomography (PET) with 2-deoxy-2-[¹⁸F]fluoro-D-glucose (FDG) as tracer may be used to depict hypermetabolism, as FDG acts as a glucose analogue [5]. Studies have shown the usefulness of contrast-enhanced CT or MRI and FDG-PET for monitoring the short-term response following both chemotherapy and radiotherapy [2,6,7]. In dynamic FDG-PET (D-PET), as opposed to conventional static FDG-PET, the spatiotemporal distribution of FDG may be depicted, which opens for imaging of both vascular and metabolic features [8–11]. Furthermore, D-PET has shown a promising potential for response assessment [10,12–15].

Functional imaging has a distinct advantage over biopsy-based assays, as tumor heterogeneity is directly available from the voxelwise distribution of

image parameters. However, single parameters such as the maximum standard uptake value (SUV_{max}) following FDG-PET examinations are still most common [16], while tumor heterogeneity in, e.g. SUV has been explored in much less detail.

In this work, we have used contrast-enhanced cone beam CT (CE-CBCT) and D-PET to assess changes in image parameters of canine head and neck tumors during the course of fractionated radiotherapy. CE-CBCT was performed at the treatment unit, facilitating fast response assessment with the patient already scheduled for treatment. We compare image parameters derived from the different modalities and discuss their potential clinical role.

Material and methods

Animals and treatment

Three companion dogs with spontaneous head and neck tumors were investigated in the present study, which study was approved by the National Committee on Animal Research. Written informed consent was obtained from the dogs' owners. The animals have been described previously [9]. Tumors were located in the right (patient A) and left (patient C) maxilla and in the right nasal cavity (patient B). The tumor volumes prior at the start of radiotherapy were 14 (A), 25 (B), and 65 (C) cm^3 . Tumor histological subtypes were plasma cell tumor (A), adenocarcinoma (B), and fibrosarcoma (C).

The dogs were treated with curative intent at an Elekta Synergy linear accelerator (Elekta AB, Stockholm, Sweden), equipped with a CBCT system (XVI). Fractionated intensity-modulated radiotherapy (IMRT) using 6 MV photons with a total dose 40–46 Gy was given in 10 fractions over two weeks. The dogs were positioned in prone position on a vacuum cushion at both treatment and imaging (see below). All imaging and treatments were performed under general anesthesia.

Imaging

CE-CBCT imaging with Omnipaque 300 mg/ml at a dose of 600 mg/kg was performed at five of the treatment sessions (no. 1, 3, 5, 7 and 10) using the linac-mounted XVI system [17,18]. Here, a CBCT scan was taken before manual contrast injection, and a second scan was started one minute post-injection (p.i.). The total duration of the CBCT scans was about one minute. The reconstructed axial CBCT images had 270×270 voxels with voxel size $1 \times 1 \times 1$ mm. The images were analyzed using custom made software in IDL (Exelis VIS, Boulder, CO, USA), where the pre-contrast images were subtracted from the post-contrast images. This difference image series

thus depicts the amount of contrast agent in tissue, where the contrast enhancement is given in Hounsfield units (HU). As contrast was injected manually, there may have been variations between fractions in injection time and injected volume. The difference images were thus normalized according to the normal tissue contrast enhancement.

Dynamic FDG-PET/CT was performed at a Siemens Biograph 16 scanner (Siemens AG, Munich, Germany). An FDG activity per body weight of roughly 6 MBq/kg was administered intravenously using a manual syringe. The scan duration was 45 minutes, with the sampling rate varying from 1/15 to 1/120/s. The longitudinal field of view (FOV) was 16 cm and the images were reconstructed with a slice resolution of 2–3 mm and an in-plane resolution of 5.5 mm, using three-dimensional (3D) OSEM iterative reconstruction (four iterations, eight subsets) and a Gaussian convolution kernel with FWHM = 5.0 mm. PET/CT was performed three days prior to treatment ('Pre'), after five fractions of radiotherapy ('Mid') and four months (four weeks for patient A) after treatment ('Post'). As for CBCT, to account for unintended variations in injected FDG, the uptake in normal tissue was used as a reference. The standard uptake value (SUV), normalized to body weight, was used as a measure of FDG uptake. Two metrics were extracted from the dynamic FDG-PET series; SUV_E and SUV_L . The former represents the mean uptake during the first two minutes of the dynamic acquisition, while the latter is the mean uptake during the last five minutes of the uptake.

Analysis

The tumor at each imaging session was manually delineated. For a given image, the full distribution of voxel values within the tumor outline was extracted. In the data presentation, main emphasis has been on the median value, as this is the best compromise of the tumor tissue as a whole. Furthermore, the 5th, 25th, 75th, and 95th percentiles were also extracted. First order linear regression was used for analyzing trends in the CBCT images during fractionated radiotherapy. χ^2 -tests were used to assess differences in the voxel value histograms. A significance level of $p = 0.05$ was chosen.

Results

Contrast-enhanced cone beam computed tomography

The contrast enhancement pattern, overlaid pre-contrast CBCT images, is shown in Figure 1 for all cases at five different treatment fractions. For each case, by inspecting the contrast enhancement pattern, the tumor may clearly be distinguished from the

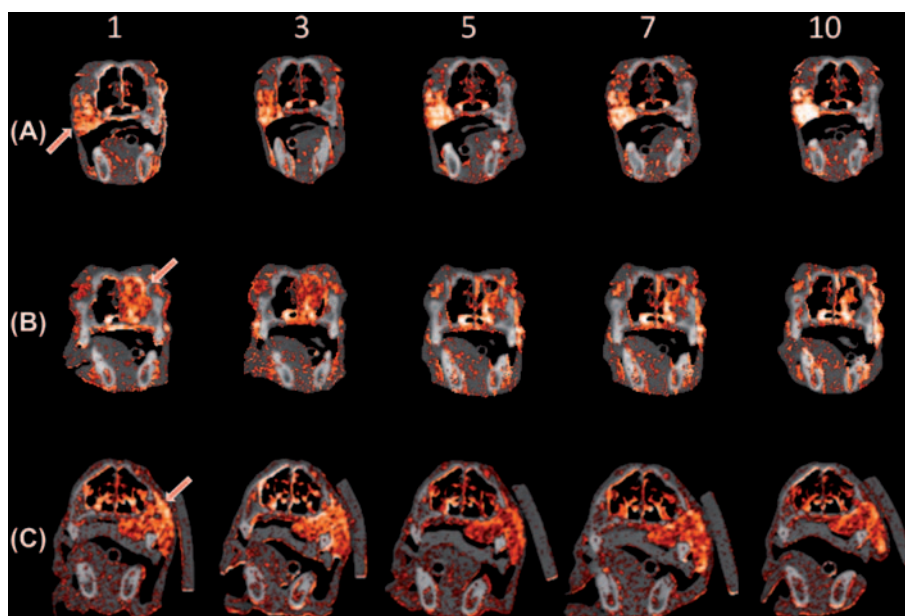


Figure 1. Contrast-enhanced cone beam CT images of patients A–C. The numbers corresponds to the treatment fractions where imaging was performed. The tumor is indicated by an arrow. The contrast enhancement window was [10,100] HU.

normal tissue. For Case A, the tumor was particularly prominent in the CE-CBCT images. For case B, the tumor regressed markedly during the fractionated treatment, but the remaining tumor tissue showed a pronounced enhancement. For case C, little or no changes could be seen in the images during the course of therapy.

The intra-tumor contrast enhancement during the course of radiotherapy is given in Figure 2. Here, the median and the 5th, 25th, 75th and 95th percentile are given to illustrate the distribution of values for a given tumor at a given fraction. A significant increase in median contrast enhancement per treatment fraction of 4.2 HU and 4.5 HU was found for case A and B, respectively, using first order linear regression. For case C, a non-significant decrease in median tumor enhancement during the course of therapy was found. The intra-tumor contrast enhancement histogram obtained prior to treatment was compared with the histograms from the different treatment fractions using the χ^2 -test. For case A, the histograms obtained at all treatment fractions were significantly different from the histogram prior to treatment. For case B, significant differences were found for fractions 5, 7, and 10, while for case C, significant differences were found for fractions 6 and 10.

Dynamic FDG-PET

Figure 3 shows DPET images for the early and late acquisition phase for all cases prior to, during and after fractionated therapy. For each case and session,

quite similar tumor extensions for were found for images acquired during the early and late acquisition phase. Also, rather small changes could be seen comparing images acquired prior to and during treatment. For case A and B, small changes were observed throughout, but case C showed a reduction in both tumor size and FDG uptake after treatment.

The temporal uptake patterns, given as the dependence of the median SUV on the time p.i., in the three different tumors prior to treatment showed substantial variations (Supplementary Figure 1, available online at <http://informahealthcare.com/doi/abs/10.3109/0284186X.2013.812800>). Case A exhibited an extremely pronounced vascular peak with an SUV of roughly 11 at about 30 s p.i. For case B and C, rather small vascular peaks could be seen. In the late uptake phase, case B showed a high and persistent increase in SUV, case C showed a slow but persistent increase, while case A plateaued already 10 minutes p.i.

The intra-tumor SUV pre-, mid- and post-radiotherapy is given in Figure 4. Here, the median and the 5th, 25th, 75th and 95th percentile are given to illustrate the SUV distribution. For case A, median SUV_E was higher than median SUV_L at all imaging sessions, while median SUV_L was higher than median SUV_E at five of six sessions for the other two cases. The changes in SUV_E and SUV_L from pre- to mid- to post-therapy were not systematic. For instance, median SUV_E increased from pre- to mid-therapy for cases A and B, while little or no change was observed for case C. Median SUV_L decreased from mid- to post-therapy with 43% for case C, while a 75% increase was seen for case B. For all cases, the

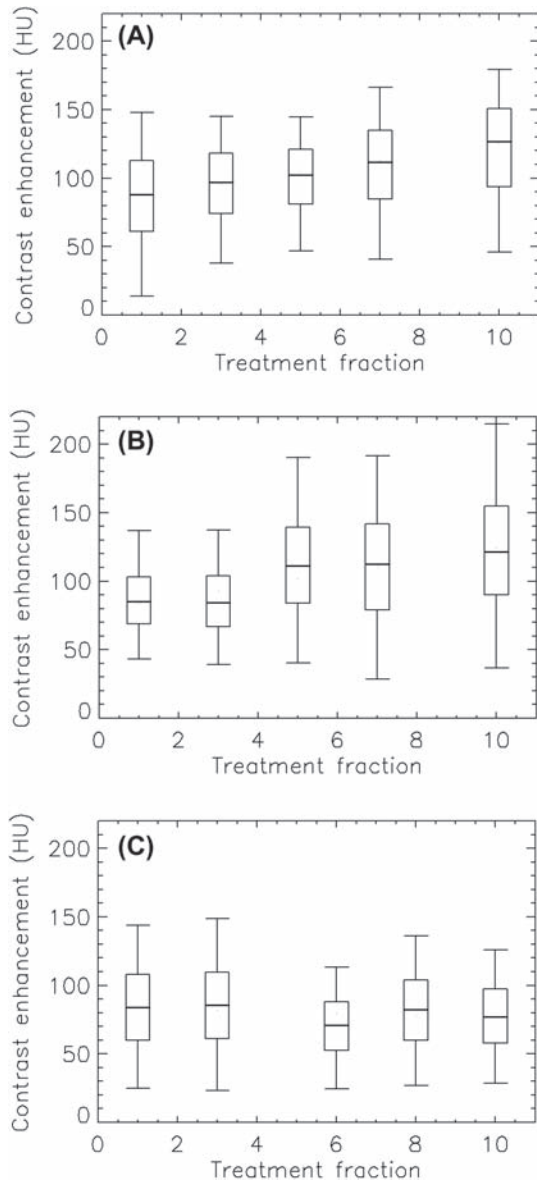


Figure 2. Box plot of showing the distribution of contrast enhancement values in the tumor as a function of treatment fraction for patients A–C. The thick line shows the median, the box covers the 25th to the 75th percentile, while the bars indicate the 5th and the 95th percentile.

intra-tumor histograms obtained at prior to, during and after treatment were all significantly different from each other, both for SUV_E and SUV_L .

Discussion

In this work, we have used CE-CBCT and DPET for tumor depiction and treatment monitoring during and after fractionated radiotherapy of canine head and neck tumors. There was a clear resemblance between the CE-CBCT and DPET images, and all images showed about the same tumor extensions in the patients. This is due to that both vascular

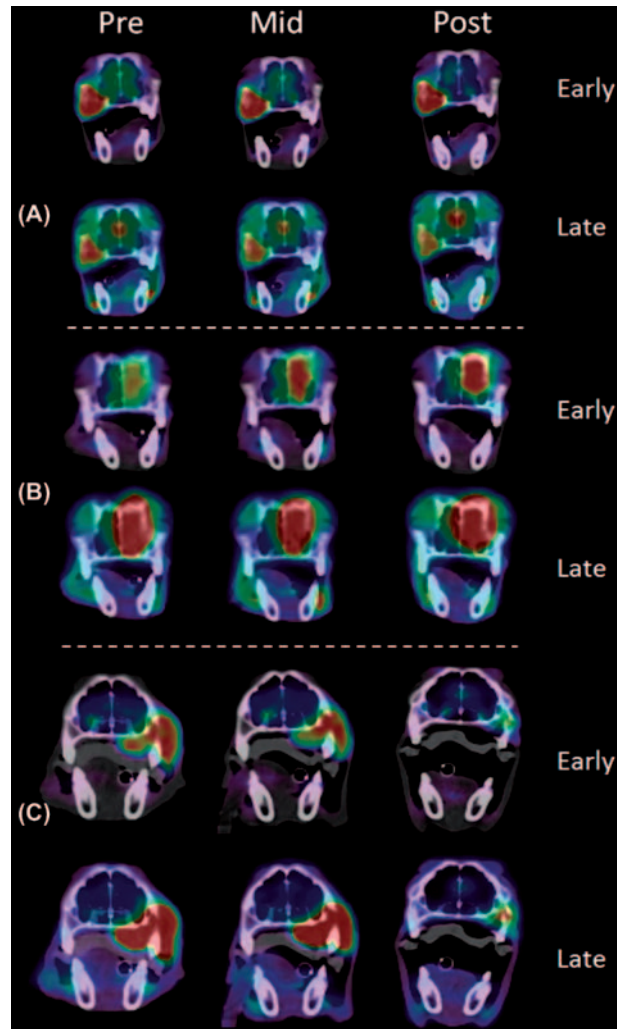


Figure 3. FDG-PET/CT images of patients A–C taken pre-, mid- and post-therapy. Images acquired in the early (0–2 min p.i.) and late (40–45 min p.i.) phase of the dynamic acquisition are shown. The SUV window was [0.5, 6].

and metabolic features may be prominent in solid tumors, although these features are not necessarily significantly correlated voxel-by-voxel [19,20]. Although the study is limited by few patients, it illustrates the attractiveness of doing multi-parameter, multi-modal imaging for assessing therapy-induced tumor alterations.

Conventional therapy response evaluation may be performed according to the RECIST criteria [1], where a partial response is defined as at least 30% reduction in tumor diameter compared to baseline. Tumor volume assessment was not a key issue in the current work, although the tumor was delineated at every imaging session. Patient B showed a partial response during radiotherapy (but had progressive disease after treatment), while patient C showed a partial response comparing the baseline scan with the post-therapy scan. Patient A exhibited more or

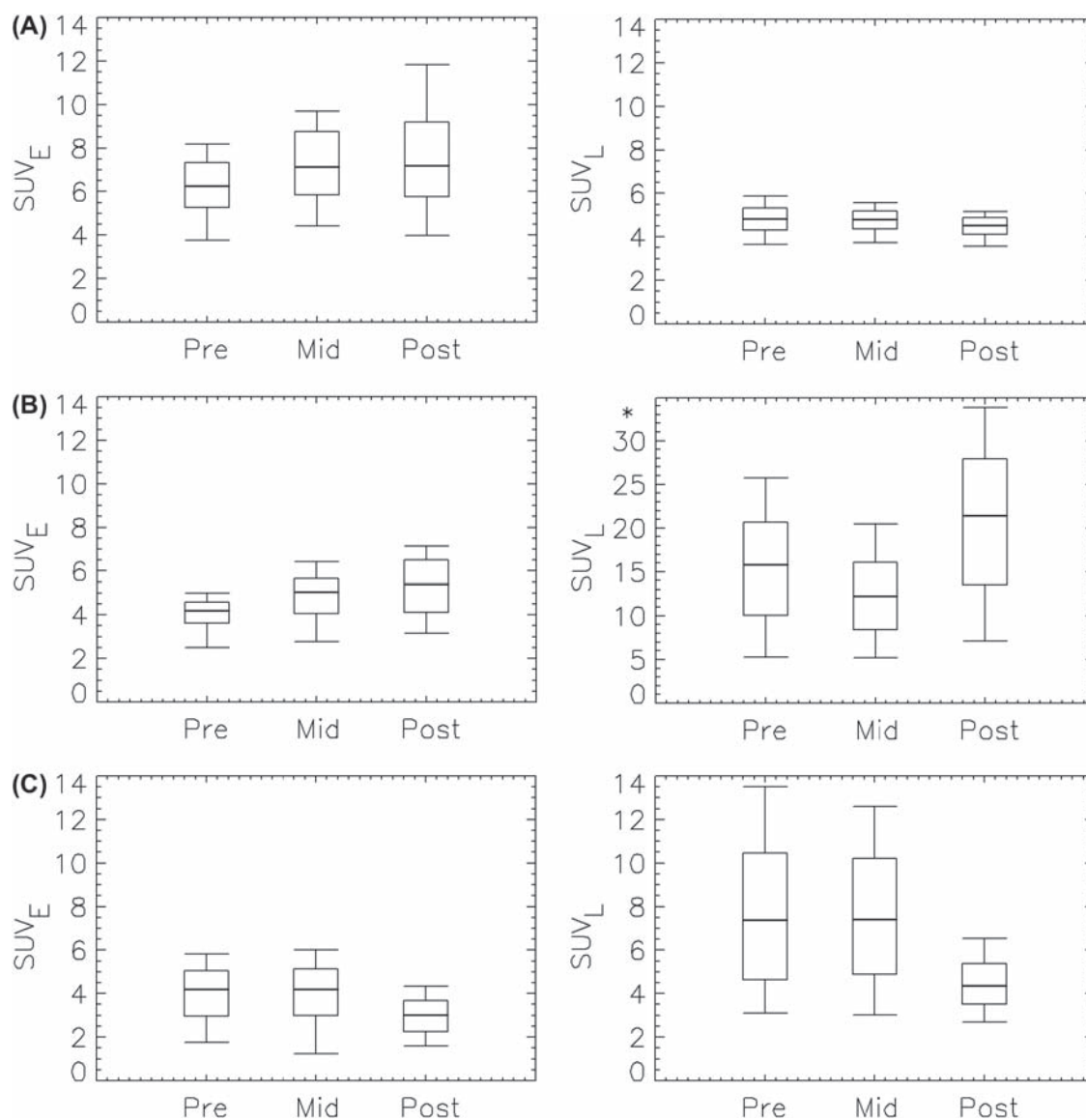


Figure 4. Box plot of showing the distribution of PET uptake values in the tumor pre-, mid- and post-therapy for patients A-C. The thick line shows the median, the box covers the 25th to the 75th percentile, while the bars indicate the 5th and the 95th percentile. *Please note different ordinate scaling.

less stable disease throughout. In the RECIST guidelines, FDG-PET was also recognized a potential response marker, but only by using standard radiological procedures (positive vs. negative PET finding). In the review leading to the PET Response Criteria in Solid Tumors (PERCIST) guidelines [2], the limitations of using anatomical tumor changes was discussed. In that work, the liver was recommended as the reference tissue in FDG-PET studies to account for, e.g. poor intravenous injection and inaccurate radiotracer dose calibration. Here, a partial metabolic response (PMR) was defined when the FDG-uptake dropped by more than 30%. If we use the median tumor SUV_L as the relevant metric, only case C showed PMR. It should be noted that the

median tumor contrast enhancement, as assessed by CE-CBCT, for patients A and B increased by more than 40 HU (more than 40%) during the full course of therapy. An increase in contrast enhancement during radiotherapy has previously shown a positive predictive value for patients with locally advanced cervical cancer [7], and it may thus be speculated that patients A and B also showed a positive response to treatment. However, none of the tumors in the current study showed a complete response, indicating that the applied radiotherapy doses were too low.

Vascular parameters derived from DCE-CT, DCE-MRI and D-PET have shown substantial spatial correlations in previous studies [9,11,21],

showing that these imaging modalities may provide similar information. D-PET may thus be used to depict both vascular and metabolic status, which is an advantage over DCE-CT and DCE-MRI. However, D-PET scans are long, and the image resolution is low. Thus combining conventional, static PET with DCE-CT or -MRI may be an option. However, full volumetric dynamic CT scanning requires state-of-the-art CT scanners that are not readily available at radiotherapy centers. In that respect, DCE-MRI may be more straightforward, although there are still issues with respect to contrast quantification and geometric distortions. CE-CBCT may thus represent a compromise with respect to imaging of vasculature [18,22]. CBCT is now largely available throughout Western European radiotherapy centers, and, using an iodinated contrast agent and an additional scan, may provide a rapid assessment of tumor status when the patient is at the treatment unit. Although dynamic scanning is not feasible, valuable information may still be obtained from CE-CBCT, as shown in the current work. Furthermore, the contrast enhancement pattern (from CE-CBCT) and SUV_E (from D-PET) was similar, and the response data also coincided: patient A and B showed an increase, while patient C show little change, in vascular parameters derived from both modalities (Figures 2 and 4). Furthermore, median contrast enhancement and median SUV_E , obtained from adjacent imaging sessions, was significantly correlated ($r = 0.71$, $p = 0.03$, data not shown), supporting our previous work on the similarities between DCE-CT and early-phase D-PET for depicting vascular status [9].

The tumor volume at a given imaging session was significantly negatively associated with median contrast enhancement, while it was not significantly associated with SUV_E and SUV_L (data not shown). A weak but significant negative correlation between tumor volume and contrast enhancement characteristics for cervical cancers has been noted previously [23], while SUV_E was not significantly correlated with tumor volume in our previous study on DPET of soft tissue sarcomas [8]. Incidentally, in that study, we found that SUV_E was higher than SUV_L for four of 11 patients, again indicating that the passive transport of FDG may be very prominent. One may speculate that large tumors outgrow the blood supply and develop necrotic centers [24], thereby showing lower mean enhancement/ SUV_E , but tumor necrosis as such was not investigated in the current study.

We used the χ^2 -test in the current work to assess changes in intra-tumoral parameter distributions. The tests revealed that the histograms quite often varied significantly from session to session, pointing to variations in tumor heterogeneity. However, the

χ^2 -test seemed quite strict, as testing the original histograms against corresponding histograms shifted only 5–10 percentage points along the abscissa gave significant differences (data not shown). Test-retest studies, where patients have been investigated multiple times prior to treatment, have revealed a variability in PET quantitative PET parameters of typically 10%, but over 40% has been reported (see [2] and references therein). Thus, improved tests taking such variability into account when assessing intra-tumor heterogeneity are needed.

In conclusion, we have shown that imaging parameters derived from CE-CBCT and D-PET provide both overlapping and complementary information. Both vascular and metabolic parameters changed during and after treatment, and CE-CBCT should be explored in future clinical trials to elucidate the potential clinical usefulness.

Declaration of interest: The authors report no conflicts of interest. The authors alone are responsible for the content and writing of the paper.

References

- [1] Eisenhauer EA, Therasse P, Bogaerts J, Schwartz LH, Sargent D, Ford R, et al. New response evaluation criteria in solid tumours: Revised RECIST guideline (version 1.1). *Eur J Cancer* 2009;45:228–247.
- [2] Wahl RL, Jacene H, Kasamon Y, Lodge MA. From RECIST to PERCIST: Evolving considerations for PET response criteria in solid tumors. *J Nucl Med* 2009;50(Suppl 1):122S–50S.
- [3] Miles KA. Tumour angiogenesis and its relation to contrast enhancement on computed tomography: A review. *Eur J Radiol* 1999;30:198–205.
- [4] Brix G, Griebel J, Kiessling F, Wenz F. Tracer kinetic modeling of tumour angiogenesis based on dynamic contrast-enhanced CT and MRI measurements. *Eur J Nucl Med Mol Imaging* 2010;37(Suppl 1):S30–51.
- [5] Zhu A, Marcus DM, Shu HK, Shim H. Application of metabolic PET imaging in radiation oncology. *Radiat Res* 2012;177:436–48.
- [6] Hatt M, van Stiphout R, le Pogam A, Lammering G, Visvikis D, Lambin P. Early prediction of pathological response in locally advanced rectal cancer based on sequential 18F-FDG PET. *Acta Oncol* 2013;52:619–26.
- [7] Mayr NA, Yuh WT, Jajoura D, Wang JZ, Lo SS, Montebello JF, et al. Ultra-early predictive assay for treatment failure using functional magnetic resonance imaging and clinical prognostic parameters in cervical cancer. *Cancer* 2010;116:903–12.
- [8] Rusten E, Rodal J, Revheim ME, Skretting A, Bruland OS, Malinen E. Quantitative dynamic (18)FDG-PET and tracer kinetic analysis of soft tissue sarcomas. *Acta Oncol Epub* 2012 Dec 3.
- [9] Malinen E, Rodal J, Knudtsen IS, Sovik A, Skogmo HK. Spatiotemporal analysis of tumor uptake patterns in dynamic (18)FDG-PET and dynamic contrast enhanced CT. *Acta Oncol* 2011;50:873–82.
- [10] Roe K, Aleksandersen TB, Kristian A, Nilsen LB, Seierstad T, Qu H, et al. Preclinical dynamic 18F-FDG PET-tumor

- characterization and radiotherapy response assessment by kinetic compartment analysis. *Acta Oncol* 2010;49: 914–21.
- [11] Mullani NA, Herbst RS, O'Neil RG, Gould KL, Barron BJ, Abbruzzese JL. Tumor blood flow measured by PET dynamic imaging of first-pass 18F-FDG uptake: A comparison with 15O-labeled water-measured blood flow. *J Nucl Med* 2008;49:517–23.
- [12] Revheim ME, Kristian A, Malinen E, Bruland OS, Berner JM, Holm R, et al. Intermittent and continuous imatinib in a human GIST xenograft model carrying KIT exon 17 resistance mutation D816H. *Acta Oncol* 2013;52: 776–82.
- [13] Cochet A, Pigeonnat S, Khoury B, Vrigneaud JM, Touzery C, Berriolo-Riedinger A, et al. Evaluation of breast tumor blood flow with dynamic first-pass 18F-FDG PET/CT: Comparison with angiogenesis markers and prognostic factors. *J Nucl Med* 2012;53:512–20.
- [14] Vriens D, de Geus-Oei LF, Heerschap A, van Laarhoven HW, Oyen WJ. Vascular and metabolic response to bevacizumab-containing regimens in two patients with colorectal liver metastases measured by dynamic contrast-enhanced MRI and dynamic 18F-FDG-PET. *Clin Colorectal Cancer* 2011;10:E1–5.
- [15] Dunnwald LK, Doot RK, Specht JM, Gralow JR, Ellis GK, Livingston RB, et al. PET tumor metabolism in locally advanced breast cancer patients undergoing neoadjuvant chemotherapy: Value of static versus kinetic measures of fluorodeoxyglucose uptake. *Clin Cancer Res* 2011;17: 2400–9.
- [16] Fuss M. Strategies of assessing and quantifying radiation treatment metabolic tumor response using F18 FDG Positron Emission Tomography (PET). *Acta Oncol* 2010; 49:948–55.
- [17] Sovik A, Rodal J, Skogmo HK, Lervag C, Eilertsen K, Malinen E. Adaptive radiotherapy based on contrast enhanced cone beam CT imaging. *Acta Oncol* 2010; 49:972–7.
- [18] Rodal J, Sovik S, Skogmo HK, Knudtsen IS, Malinen E. Feasibility of contrast-enhanced cone-beam CT for target localization and treatment monitoring. *Radiother Oncol* 2010;97:521–4.
- [19] Miles KA, Williams RE. Warburg revisited: Imaging tumour blood flow and metabolism. *Cancer Imaging* 2008;8:81–6.
- [20] Goh V, Shastry M, Engledow A, Kozarski R, Peck J, Endozo R, et al. Integrated (18)F-FDG PET/CT and perfusion CT of primary colorectal cancer: Effect of inter- and intraobserver agreement on metabolic-vascular parameters. *AJR Am J Roentgenol* 2012;199:1003–9.
- [21] Eby PR, Partridge SC, White SW, Doot RK, Dunnwald LK, Schubert EK, et al. Metabolic and vascular features of dynamic contrast-enhanced breast magnetic resonance imaging and (15)O-water positron emission tomography blood flow in breast cancer. *Acad Radiol* 2008;15:1246–54.
- [22] Igaki H, Nakagawa K, Yamashita H, Terahara A, Haga A, Shiraiishi K, et al. Contrast media-assisted visualization of brain metastases by kilovoltage cone-beam CT. *Acta Oncol* 2009;48:314–7.
- [23] Andersen EK, Hole KH, Lund KV, Sundfor K, Kristensen GB, Lyng H, et al. Pharmacokinetic parameters derived from dynamic contrast enhanced MRI of cervical cancers predict chemoradiotherapy outcome. *Radiother Oncol* 2013;107: 117–22.
- [24] Caruso R, Parisi A, Bonanno A, Paparo D, Quattrocchi E, Branca G, et al. Histologic coagulative tumour necrosis as a prognostic indicator of aggressiveness in renal, lung, thyroid and colorectal carcinomas: A brief review. *Oncol Lett* 2012;3:16–8.

Supplementary material available online

Supplementary Figure 1